

# Enhancing effect of $\text{KMnO}_4$ oxidation of carbon nanotubes network embedded in elastic polyurethane on overall electro-mechanical properties of composite

P. Slobodian<sup>a,b,\*</sup>, P. Riha<sup>c</sup>, R. Olejnik<sup>a,b</sup>, U. Cvelbar<sup>d</sup>, P. Saha<sup>a,b</sup>

<sup>a</sup>*Polymer Centre, Faculty of Technology, T. Bata University, T.G.M. 275, 76272 Zlin, Czech*

*Republic*

<sup>b</sup>*Centre of Polymer Systems, University Institute, T. Bata University, Nad Ovcimou 3685, 76001*

*Zlin, Czech Republic*

<sup>c</sup>*Institute of Hydrodynamics, Academy of Sciences, Pod Patankou 5, 166 12 Prague 6, Czech*

*Republic*

<sup>d</sup>*Jozef Stefan Institute F4, Jamova cesta 39, 1000 Ljubjana, Slovenia*

---

## ABSTRACT

The effect of functionalization of multi-walled carbon nanotubes using  $\text{KMnO}_4$  oxidation and oxygen plasma treatment on the electrical resistance of nanotube network/polyurethane composite subjected to elongation has been studied. The layered composite is prepared by taking a non-woven polyurethane filtering membrane which is made by electrospinning, enmeshing it with carbon nanotubes and melding them into one. The testing has shown tenfold composite resistance increase for the composite prepared from  $\text{KMnO}_4$  oxidized nanotubes in comparison to the network prepared from pristine nanotubes. The evaluated sensitivity of the treated

composite in terms of the gauge factor increases linearly with strain from values around 5 at the start of deformation to nearly 45 at the strain 12 %. This is a substantial increase, which put the composite prepared from  $\text{KMnO}_4$  oxidized nanotubes among ranges the materials and strain gauges with the highest sensitivity of electrical resistance measurement.

### *Keywords*

A. Carbon nanotubes; A. Nanocomposites; B. Electrical properties; C. Deformation; Nanotube oxidation;

---

\*Corresponding-Author: Tel.: +420 576031350; fax: +420 576031444.

E-mail address: [slobodian@ft.utb.cz](mailto:slobodian@ft.utb.cz).

## **1. Introduction**

The oxidation of carbon nanotubes (CNT) became a frequent way to enhance their chemical reactivity and extend application potentiality. Typically, the nanotube wet oxidation by the potassium permanganate ( $\text{KMnO}_4$ ) produces carboxylic acid groups (-COOH) on nanotube surface as well as a significant amount of other oxygenated functional groups such as hydroxyl (-OH) and carbonyl (=O) groups [1,2]. The oxidation enhances gas sensing properties of nanotubes toward organic vapors which can be attributed to better affinity of vapors to the oxidized form of nanotubes [3].

Moreover, it was found that the nanotube network made from oxidized nanotubes has

2

more uniform pore structure and dense morphology with lower porosity in comparison with networks formed by pristine nanotubes [4]. The network structure results from fine nanotube aqueous dispersion, and thus deposition of individual nanotubes and/or only small nanotube agglomerates on filtrating membrane since the presence of oxygen-containing groups facilitates the exfoliation of nanotube bundles and increases their dispersion in polar media [1,2,5].

The oxygen plasma treatment of carbon nanotubes preferentially forms hydroxyl and carboxyl groups on the surface of nanotubes, so that nanotubes can provide a strong affinity to liquid molecules and self-disperse into a liquid medium [6-8]. The plasma treatment has the advantage of being non-polluting and the amount of functional groups grafted on the nanotubes surface can be tailored.

The aim of this paper is to study the effect of nanotube oxidation on electromechanical properties of nanotube network/polyurethane composite both in the course of monotonic elongation and when elongating/relaxing cycles are imposed. In this respect, the main achievement is a multiple increase of gauge factor evaluating electromechanical properties of the composite due to  $\text{KMnO}_4$  oxidation of nanotubes.

## **2. Experimental**

### *2.1 Materials*

Multi-walled carbon nanotubes (MWCNTs) BAYTUBES C70 P produced by chemical vapor deposition were supplied by the Bayer MaterialScience AG, Germany

(C-purity > 95 wt.%, outer mean diameter ~13 nm, inner mean diameter ~4 nm, length > 1  $\mu\text{m}$  and declared bulk density of MWCNT of agglomerates of micrometric size 45-95  $\text{kg}/\text{m}^3$ ). The oxidized MWCNTs were prepared in a glass reactor with a reflux condenser filled with 250  $\text{cm}^3$  of 0.5M  $\text{H}_2\text{SO}_4$ , into which 5g of  $\text{KMnO}_4$  (potassium permanganate) as oxidizing agent and 2g of MWCNTs were added. The dispersion was sonicated at 85°C for 15 hours using thermostatic ultrasonic bath (Bandelin electronic DT 103H). The dispersion was filtered and MWCNTs washed with concentrated HCl to remove  $\text{MnO}_2$ . Besides MWCNT functionalization by the potassium permanganate, the portion of MWCNTs was treated by low temperature oxygen plasma generated in an inductively coupled radiofrequency discharge at 27.12 MHz in a commercially available  $\text{O}_2$  gas at the pressure 50 Pa for 10 minutes.

Nanotubes were used for the preparation of three aqueous pastes: 1.6 g of MWCNTs (either pristine,  $\text{KMnO}_4$  oxidized or  $\text{O}_2$  plasma oxidized) and ~50 ml of deionized water was mixed with a mortar and pestle. The pastes were then diluted in deionized water with sodium dodecyl sulfate (SDS) and 1-pentanol. Consequently, an aqueous solution of NaOH was added to adjust the pH at value of 10. The final nanotube concentration in suspensions was 0.3 wt.%, concentration of SDS and 1-pentanol 0.1M and 0.14M, respectively. The suspensions were sonicated in an apparatus from “Dr. Hielscher GmbH” (ultrasonic horn S7, amplitude 88  $\mu\text{m}$ , power density 300  $\text{W}/\text{cm}^2$ , frequency 24 kHz) for 2 hours and with temperature of ca 50°C.

MWCNT network (buckypaper) (MWCNT-N) was prepared by nanotube dispersion vacuum filtration through polyurethane (PU) membrane prepared by

4

technology of electrospinning in cooperation with the SPUR Company a.s. (Czech Republic) [9]. The other networks were prepared from treated MWCNTs in the same way as MWCNT-N. These networks are thereafter denoted MWCNT-N<sub>(KMnO<sub>4</sub>)</sub> and MWCNT-N<sub>(O<sub>2</sub> plasma)</sub>.

For an electrospinning process producing PU non-woven filters, the granulated polyurethane elastomer Desmopan DP 2590A supplied by Bayer MaterialScience was used. Desmopan DP 2590A is a polyester based thermoplastic polyurethane which is produced using monomers 4,4'-Methylenebis(phenyl isocyanate), polyadipate (1,4-butanediol/adipic acid) and 1,4-butanediol as a chain extender. The limited PU properties provided by the manufacture specify density 1210 kg/m<sup>3</sup>, melt temperature 210 – 230 °C, mold temperature 20 - 40 °C and strain at break 440 %.

The polyurethane granules were dissolved in a mixture of dimethyl formamide/methyl isobutyl ketone (Penta Chemikalie, Czech Republic) with volume ratio 3:1. The polymer weight concentration was adjusted to 16 % (w/v) and the mixture electric conductivity to 30 μs/cm by adding NaCl in order to optimize the process. The distance of the steel multi-jet spinning electrode and the steel plate as the collecting electrode of the electrospinning equipment (SPUR a.s., Czech Republic) was 180 mm, Fig. 1. The total number of nozzles was 18, the length of nozzles 30 mm, the distance between nozzles 20 mm, the nozzle internal diameter 1.2 mm and the outer diameter 2.2 mm. The electric voltage was set to 75 kV (Matsusada DC power supply), the temperature 21 ± 2 °C, the relative humidity 35 ± 2.5% and the flow rate of fresh polymeric solution in one nozzle 1.6 μl/min. The final thickness of PU

non-woven filters was about 200  $\mu\text{m}$ .

The filtered MWCNT networks were washed several times by deionized water and methanol in situ and dried between two glass micro-fiber filter papers at 40°C for 24 hours. Polyurethane filter and MWCNT network form the layered structure which was melt welded (at 175 °C) onto the surface of PU tensile test specimen for extension/resistance tests. The partial infiltration of MWCNTs into the filter pores creates an effective interlocking of MWCNT network layer with PU filter which even strengthens when the porous filter is transformed into the polymeric film in the course of compression melt welding.

## *2.2 Instruments*

Pristine,  $\text{KMnO}_4$ , and oxygen plasma-oxidized MWCNTs were analyzed via transmission electron microscopy (TEM) using microscope JEOL JEM 2010 at the accelerating voltage of 160 kV. The sample for TEM was fabricated on 300 mesh copper grid with a carbon film (SPI, USA) from MWCNT dispersion in acetone prepared by ultrasonication, which was deposited on the grid and dried. The structure of MWCNT networks, PU filtering membrane and MWCNT/PU composites were analyzed by scanning electron microscope (SEM) Vega LMU, produced by Tescan Ltd. The samples were deposited on carbon targets and covered with a thin Au/Pd layer. For the observations the regime of secondary electrons was chosen. The content of oxygen in each form of MWCNT networks was detected with help of X-ray

spectroscopy (EDX) which is among accessories of SEM microscope. Thermogravimetric analyses (TGA) of MWCNT samples were carried out using thermogravimeter Setaram Setsyt Evolution 1200. The samples were examined under inert atmosphere of helium (5.5 purity, SIAD TP); the gas flow was 30 cm<sup>3</sup>/min at the pressure of 101.325 kPa (i.e. 30 sccm) for all experiments. A platinum crucible was used for the sample, the weight of which was about 4 mg. The temperature was increased from ambient up to 1200 °C at the rate of 20 °C/min.

### *2.3 Measurement of electrical resistance*

The purpose of this study is to investigate the change of electrical resistance of different MWCNT network/PU composites in extension. The resistance change of the composite is monitored by a two-point technique by means of Wheatstone bridge (the resistance of the bridge resistors  $R_1 = 120 \Omega$ ,  $R_3 = 119 \Omega$ ,  $R_2 = 0-1000 \Omega$  and supply voltage 5V), the multimeter METEX M-3860D and voltage supply METEX AX 502. The time-dependent resistance change of composite was measured by means of the Vernier LabQuest Interface System connected to the Differential Voltage Probe and the Wheatstone bridge with sampling frequency 10 and 100 Hz.

For attachment of two copper electrodes to the MWCNT network of the composite samples a screw mechanism was used. The screw tightening was terminated when there was no decrease of network resistance. In that manner, the contact resistance between the network and copper electrodes is controlled and the initial electrical resistance of the system is equally adjusted before the first sample elongation. Initially

the network under the screw was pasted by Ag colloid electro-conductive paint Dotite D-550 (SPI Supplies) to decrease the contact resistance. However, the pasting turned out ineffective since no change of the contact resistance was observed. Moreover, the paint crackled and crumbled away in the course of composite elongation.

### 3. Results

A detailed view of the structure of individual nanotubes and the cluster of nanotubes obtained by means of the transmission electron microscopy (TEM) is shown in Fig. 2a and b, respectively. The nanotube outer and inner diameter is about 20 nm and 4-10 nm, respectively. The multi-wall consists of about 15 rolled layers of graphene. There are also defects obstructing nanotube interior which are commonly seen in MWCNT structures [13]. When the cluster of pristine nanotubes is compared with the cluster of wet oxidized nanotubes in Fig. 2c, the change of the tube length is visible. Oxidation of MWCNT by  $\text{KMnO}_4/\text{H}_2\text{SO}_4$  mixture causes nanotubes shortening, creation of defect sites and opened ends. Small amount of amorphous carbon after the  $\text{KMnO}_4$  oxidation process can be also expected [1] although other report shows that oxidation by  $\text{KMnO}_4$  in an acidic suspension provides nanotubes free of amorphous carbon [2]. Oxidation by  $\text{KMnO}_4$  can be easily controlled. The disadvantage is that created  $\text{MnO}_2$  must be dissolved by concentrated HCl acid [1]. Finally, it is necessary stated that also the used high-energy ultrasound can cause similar effects as oxidation, that is, reduction of nanotube length with ends open by MWCNT shortening [1,2]. In our case the energy-dispersive X-ray spectroscopy

8



proves an increase of oxygen content on the surface of MWCNT-N<sub>(KMnO<sub>4</sub>)</sub> compared to pristine MWCNT-N from 2.8 at.% to 11.9 at.% ; O/C ratio thus increases from 0.03 to 0.14. In the case of plasma treated tubes it is also obvious from TEM analyses that CNT shortening occurred, Fig. 2 d. However, the plasma treatment does not increase oxygen content on CNT surface as significantly as KMnO<sub>4</sub> oxidation process. The oxygen content is 6.3 % and O/C ratio 0.07. These results can be supplemented by additional ones of the thermogravimetric analyses, Fig. 3. As can be seen from the figure, pure MWCNTs show hardly any degradation in the range of temperature up to 700°C; only very small mass loss of ca 2.5 wt. % was observed at the highest temperature values. This is probably caused by decomposition of amorphous carbon contained in the pristine nanotubes together with functional groups like O-C=O or C-O [11]. The similar nanotube degradation as pristine nanotubes show O<sub>2</sub> plasma treated MWCNTs except a slight increase of decomposed material at 700°C to ca 3.3 wt. %. It confirms only small increase of functional groups attached onto MWCNT surface during plasma treatment. On the other hand KMnO<sub>4</sub> oxidized tubes show higher weight loss at 700°C, ca 9.8 wt. %. The increase is probably caused by a higher content of functional groups, mainly acidic sites but also –OH or C=O groups [14], which are expected to be introduced during oxidation process.

The oxidized nanotubes create smaller entangled bundles (aggregates) in solution than observed for pristine CNTs. Kastanis et al. [15] tested three different oxidizing agents, namely ammonium hydroxide/hydrogen peroxide, sulfuric acid/hydrogen peroxide and hot nitric acid. They found that the increasing oxygen content on the

surface of nanotubes leads to MWCNT networks with more uniform pore structure and dense morphology with lower porosity in comparison with pristine MWCNT networks. It indicates better nanotube dispersion in the aqueous suspension during filtration process and network formation when nanotubes are deposited individually or as a small CNT bundles. The similar finding was described in our previous paper using different kind of MWCNTs [4].

Fig. 4 shows SEM micrographs of upper surface of entangled MWCNT network of pristine,  $\text{KMnO}_4$  oxidized and  $\text{O}_2$  plasma treated nanotubes. The network of oxidized MWCNT and  $\text{O}_2$  plasma treated nanotubes seems to be densely packed than the network of pristine nanotubes. The quantitative difference in MWCNT network structures was determined on basis of the determination of their porosities,  $\phi$ . The calculated porosity values were 0.71 (MWCNT-N), 0.63 (MWCNT-N<sub>(KMnO<sub>4</sub>)</sub>) and 0.67 (MWCNT-N<sub>(O<sub>2</sub> plasma)</sub>). For the calculation, the relation  $\phi = 1 - \rho_{net}/\rho_{MWCNT}$  was used. The  $\rho_{net}$  value, the measured apparent density of the network, was  $0.38 \pm 0.01 \text{ g/cm}^3$  (pristine),  $0.48 \pm 0.01 \text{ g/cm}^3$  ( $\text{KMnO}_4$  oxidized) and  $0.43 \pm 0.02 \text{ g/cm}^3$  ( $\text{O}_2$  plasma treated). The measured average density of nanotubes  $\rho_{MWCNT} = 1.3 \text{ g/cm}^3$ .

The electrical resistance of MWCNT network is mainly affected by the resistance of inter-tube contacts and the number of contacts, since the conductive nanotubes are short (max. several micrometers) and cannot create a continuous conductive path [16,17]. However, according to our measurement, the oxidation also increases the network resistance [4].

The measured resistivity of MWCNT network structures was  $0.068 \pm 0.005 \text{ } \Omega\text{cm}$  for

MWCNT-N,  $0.317 \pm 0.010 \text{ } \Omega\text{cm}$  for MWCNT-N<sub>(KMnO<sub>4</sub>)</sub> and  $0.071 \pm 0.004 \text{ } \Omega\text{cm}$  for MWCNT-N<sub>(O<sub>2</sub> plasma)</sub>. The resistance of the nanotube contacts in the network,  $R_{contact}$ , calculated by means of the following model [16],

$$R_{contact} = \frac{\rho_{net} A^2}{m} \frac{\pi}{16d} \varphi R \quad (1)$$

is  $3.1 \pm 0.4 \text{ k}\Omega$  (MWCNT-N),  $18.2 \pm 0.8 \text{ k}\Omega$  (MWCNT-N<sub>(KMnO<sub>4</sub>)</sub>) and  $4.0 \pm 0.3$  (MWCNT-N<sub>(O<sub>2</sub> plasma)</sub>) for the average nanotube diameter of 13 nm. The letters  $m$ ,  $A$  and  $d$  in Eq. (1) denote the weight of the sample, its cross section perpendicular to electrical current direction and average CNT diameter, respectively.  $R$  denotes the resistance of the whole network and  $\varphi$  the volume fraction of MWCNT defined as  $\varphi = 1 - \phi$ , where  $\phi$  denotes the porosity specified above for MWCNT-N, MWCNT-N<sub>(KMnO<sub>4</sub>)</sub> and MWCNT-N<sub>(O<sub>2</sub> plasma)</sub>. The value of  $R_{contact}$  is more than five times higher for oxidized nanotubes in comparison to pristine ones but only a small increase of the contact resistance was calculated for plasma treated nanotubes compared to the contact resistance of pristine nanotubes. The role may play the content of oxygenated functional groups.

The non-woven filtering membrane made from thermoplastic polyurethane for CNT dispersion vacuum filtration was prepared by technology of electrospinning. The scanning electron microscope (SEM) micrograph of PU filter is shown in Fig. 5a. PU fibers are straight with a relatively smooth surface. The fiber diameter ranges between  $0.05\text{-}0.39 \text{ } \mu\text{m}$  (average diameter  $0.14 \pm 0.09 \text{ } \mu\text{m}$ ). The main pore size is around  $0.2 \text{ } \mu\text{m}$ .

In the course of CNT dispersion filtration PU filter pores allow partial infiltration of nanotubes into the filter at the beginning of filtration. When the pores are filled with nanotubes, the filter cake (nanotube entangled network) is formed above the filter surface. This partial infiltration of MWCNTs into the filter pores creates an effective mechanical interlocking of MWCNT network layer with PU filter. The final structure of strain sensitive composite is formed in the course of molding at 175 °C when the layer of pure polyurethane stem from the melted PU filtering membrane and the layer of pure MWCNT network is embedded into the polymer. Thus the final structure of the layered composite consists of three layers. The first electrically non-conducting layer is the supporting pure PU layer. The second already conductive interlayer is the particulate MWCNT/PU nanocomposite film which is formed during membrane melting so that the surface nanotubes of the network are enclosed by polymer and embedded in PU layer. The third conductive layer is formed by pure MWCNT network which due to firm link with the polymer is reversibly stretchable. The second and third layers form the sensitive part of layered, longitudinally conductive MWCNT-N/PU composite. The typical thickness of PU layer is 2 mm, the interlayer 3  $\mu\text{m}$  and the pure MWCNT network layer 30  $\mu\text{m}$ .

SEM micrograph of the upper surface of MWCNT-N/PU composite after washing out the pure MWCNT network is shown in Fig. 5b. The cross-section through the same composite with interlayer of embedded MWCNTs into the polyurethane is shown in Fig. 5c.

The sample of different MWCNT-N/PU composite of the size 10x50 mm can be

easily melt welded onto the surface of PU tensile test specimen (dog-bone shaped) for extension and resistance tests [18], see Fig. 5d. Shape and dimensions of the test specimen are chosen according to standard EN ISO 3167, with a thickness of 2 mm.

The extension of all kinds of prepared MWCNT/PU composites affects their electrical resistance change with strain. Fig. 6 shows seven extension/relaxation cycles in the course of step increase of tensile strain for PU composite with MWCNT-N and MWCNT-N<sub>(KMnO<sub>4</sub>)</sub>, respectively. The resistance change is defined as:  $\Delta R/R_0 = (R - R_0)/R_0$ , where  $R_0$  is the electrical resistance of the measured sample before the first elongation, and  $R$  is the resistance while elongating.  $\varepsilon$  denotes the percentage of mechanical strain, which is the relative change in length. The period of extension/relaxation cycle is 60 s. From Fig. 6 follow considerable difference in the resistance change of tested composites both with respect to the sensitivity to strain and irreversible residual changes. The increasing stress obviously enhances composite irreversible deformation. Consequently, the residual strain and the residual resistance change increases in the off-load state with increasing number of cycles. The residual resistance change is caused by deformation of conductive structure of MWCNT network which may include nanotube slippage, delamination and buckling. However, in addition to the network deformation, the network cracking may cause breaks of a portion of electric circuit with the applied stress. The residual resistance change is lower in case of MWCNT-N/PU composite than MWCNT-N<sub>(KMnO<sub>4</sub>)</sub>/PU composite. For example, in case of MWCNT/PU composite the resistance change is around 36% after elongation ~10%, while the corresponding resistance change for

MWCNT-N<sub>(KMnO<sub>4</sub>)</sub>/PU composite is about 438 %. On the other hand, the residual resistance change after load remove and 1 min relaxation is 19% and 30% in case of MWCNT-N and MWCNT-N<sub>(KMnO<sub>4</sub>)</sub>/PU composite, respectively (Fig. 6). However, the corresponding residual resistance change after relaxation is higher, about 51 % , in case of MWCNT-N<sub>(O<sub>2</sub> plasma)</sub>/PU composite.

Elongation causes a resistance change during both the up-stress and down-stress periods due to specific deformation of porous structure. The local contact forces between nanotubes decrease probably during elongation, allowing a worse contact of nanotubes and thus increase of their contact resistance. Moreover, the distance between contacts may increase during elongation owing to evoked relative motion of nanotubes, which corresponds to higher intrinsic resistance of nanotube segments between contacts. Last but not least, the elongation may also straighten the nanotubes, which results in a less contacts between nanotubes. Since the contact points may act as parallel resistors, their decreasing number causes an enhancement of MWCNT network resistance. This structure reorganization, i.e. less contact points, probably partly remains when the tensile strength is released, which may be the reason for off-load residual resistance increase. Nevertheless, the ongoing extension cycles have a stabilizing effect on the resistance-elongation dependence as observed during repeated cycles and described below.

Since the pristine and oxidized nanotubes have different porosities (0.71 MWCNT-N, 0.63 MWCNT-N<sub>(KMnO<sub>4</sub>)</sub>), the structure of networks may have influence on the different strain dependent change of resistance of composites with pristine or

oxidized nanotubes. However, this mechanical view does not explain fully the significant difference in the resistance change with elongation. The chemical treatment of nanotubes plays probably a dominant role. We have found by the energy-dispersive X-ray spectroscopy the increase of oxygen content on surface of MWCNT-N<sub>(KMnO<sub>4</sub>)</sub> compared to pristine MWCNT-N from 2.8 at.% to 11.9 at.% ; O/C ratio increases from 0.03 to 0.14. Thus the number of structural defects may increase after KMnO<sub>4</sub> treatment and affect the mechanism of electrical resistance. The oxygen atoms act as acceptors of electrons and change the density of current carriers in surface layers of MWCNTs and thus may decrease electrical conductivity of the composite made of KMnO<sub>4</sub> oxidized nanotubes. Moreover, NH groups as proton donors and oxygen in carbonyl groups of urethane and ester groups as proton acceptors in the polyester-based polyurethane affect formation of hydrogen bonding. Since MWCNT-Ns have hydroxyl, carboxyl, ketone and ether groups on their surface, these groups may play a part in forming hydrogen bonding between the polymer and MWCNT-Ns.

Besides the difference in the residual resistance change of the tested composite, a very significant difference was observed also in the sensitivity to strain. The sensitivity of strain gauge is usually measured by a gauge factor (*GF*) which is defined as the relative resistance change divided by the applied strain,  $GF = (\Delta R/R_0)/\epsilon$ . To have a high sensitivity, that is, a high change in resistance for the same strain, higher value of gauge factor is desirable. Using data presented in Fig. 6, *GF* for MWCNT-N/PU slightly increases with deformation reaching nearly constant value

$GF= 3.5$  above strain 4%. Gauge factor for MWCNT-N( $O_2$  plasma)/PU composite is very similar to the previous case with high strain  $GF$  about 4.2, Fig. 7. On the other hand, the gauge factor for MWCNT-N( $KMnO_4$ )/PU composite increases linearly with strain from values of around 5 at the beginning of deformation to nearly 44 at the strain 10.4 %, Fig. 7. The reproducibility (repeatability) of the resistance change measurement is illustrated by taking 5 measurements on each composite type. Its estimation by the error bars representing standard deviation in Fig. 7 show a reasonable values.

Figs. 8 and 9 show waveforms of the applied deformation and resistance change response for MWCNT-N/PU and MWCNT-N( $KMnO_4$ )/PU composites in three cycles. Though the resistance mechanism is apparently not reversible in the initial cycle since the relaxation curve has a residual resistance increase in the off-load state, Fig. 6, the ongoing elongation cycles have a stabilizing effect on the resistance and strain time dependence, Figs. 8 and 9. The initial residual resistance change during each cycle tends to reach immediately the final value and ensures the repeatability of the resistance-strain dependence. It indicates that during initial deformation the nanotube network gets the structure which stays more or less the same regardless the number of deformation cycles. This mechanical stabilization is favorable for the use of the composite as a sensing element of elongation, especially when the network is suitably deformed in advance.

From the comparison of waveforms in Figs. 8 and 9 is obvious that in case of MWCNT-N/PU composite the strain sinusoid and the resistance change sinusoid are



identical for the strain varying between 2.6 and 8.4 % with frequency 0.07 Hz and the resistance change varying between 10.9 % and 26.6 %, Fig. 8. On the other side, when MWCNT-N<sub>(KMnO<sub>4</sub>)</sub>/PU composite is subjected to similar cyclic deformation as the composite with pristine nanotubes (strain varies between 2.0 % and 7.9 % with frequency 0.05 Hz), the response of resistance change differs from the strain sinusoid. The resistance change is greater than in case of the composite with pristine nanotubes (the relative resistance change varies between 104.9 % and 247.8 %) and the resistance increase is faster than strain stimulation and vice versa. The short oxidized nanotubes probably lose contacts with other ones more easily with the composite elongation than the longer pristine nanotubes. On the other hand, the readjustment of oxidized nanotube network and formation of nanotube intercontacts with decreasing strain is slower than in case of composite with pristine nanotubes.

Fig. 10 demonstrates properties of MWCNT-N<sub>(KMnO<sub>4</sub>)</sub>/PU composite as well as the properties repeatability under long-lasting cyclic elongation. The frequency of strain cycle is about 1 Hz and more than 10<sup>4</sup> cycles has been monitored. The results show that the resistance change is repetitive and no composite property variation is observed. The composite has reasonable durability and reversibility of the base characteristics complying practical application requirements.

#### **4. Conclusion**

Three different kinds of MWCNT/PU composite were prepared to investigate the effect of nanotube oxidation on the modification of their mechanical and electrical

properties in the course of monotonic elongation and when elongating/relaxing cycles are imposed. The testing has shown tenfold composite resistance increase for MWCNT network prepared from  $\text{KMnO}_4$  oxidized nanotubes in comparison to the network prepared from pristine MWCNT and also  $\text{O}_2$  plasma oxidized MWCNT network. The evaluated sensitivity of MWCNT- $\text{N}_{(\text{KMnO}_4)}$ /PU composite in terms of the gauge factor increases linearly with strain from values around 5 at the start of deformation to nearly 44 at the strain 12 %. This is a substantial increase, which put the composite among the materials and strain gauges with the highest sensitivity of electrical resistance measurement. The resistance and sensitivity increase in elongation comes probably from the different porosity of networks and increased content of oxygenated functional groups detached on MWCNT- $\text{N}_{(\text{KMnO}_4)}$  surface which significantly increase contact resistance in CNT junction of network structure. The short oxidized nanotubes probably lose contacts with other ones more easily with the composite elongation than the longer pristine nanotubes. The long-lasting cyclic stretching of MWCNT- $\text{N}_{(\text{KMnO}_4)}$ /PU composite shows reasonable durability and reversibility of the composite deformation and electrical resistance complying practical application requirements.

### **Acknowledgement**

The work was supported by the Operational Program of Research and Development for Innovations co-funded by the European Regional Development Fund (ERDF), the National budget of Czech Republic within the framework of the

Centre of Polymer Systems project (reg. number: CZ.1.05/2.1.00/03.0111). The article was written with the support of the Operational Programme „Education for Competitiveness“ co-funded by the European Social Fund (ESF) and the national budget of the Czech Republic, within the „Advanced Theoretical and Experimental Studies of Polymer Systems“ project (reg. number: CZ.1.07/2.3.00/20.0104). The Fund of Institute of Hydrodynamics, no. of project AV0Z20600510, is also acknowledged for support.

## References

- [1] Hernadi K, Siska A, Thien-Nga L, Forro L, Kiricsi I. Reactivity of different kinds of carbon during oxidative purification of catalytically prepared carbon nanotubes, *Solid State Ionics* 2001;141(1):203-209.
- [2] Rasheed A, Howe JY, Dadmun MD, Britt PF. The efficiency of the oxidation of carbon nanofibers with various oxidizing agents. *Carbon* 2007;45:1072-1080.
- [3] Hussain CM, Saridara C, Mitra S. Microtrapping characteristics of single and multi-walled carbon nanotubes. *J Chromatogr A* 2008;1185(2):161-166.
- [4] Slobodian P, Riha P, Lengalova A, Svoboda P, Saha P. Multi-wall carbon nanotube networks as potential resistive gas sensors for organic vapor detection. *Carbon* 2011;49(7):2499-2507.
- [5] Datsyuk V, Kalyva M, Papagelis K, Parthenios J, Tasis D, Siokou A, Kallitsis I, Galiotis C. Chemical oxidation of multiwalled carbon nanotubes. *Carbon*

2008;46:833-840.

- [6] Kalita G, Adhikan S, Aryal HR, Umeno M, Afre R, Soga T, Fullerene (C<sub>60</sub>) decoration in oxygen plasma treated multiwalled carbon nanotubes for photovoltaic application. *Appl Phys Lett* 2008;92:063508 (3 pages).
- [7] Chen C, Ogino A, Wang X, Nagatsu M. Plasma treatment of multiwall carbon nanotubes for dispersion improvement in water. *Appl Phys Lett* 2010;96:131504 (3 pages).
- [8] Chen W, Liu X, Liu Y, Bang Y, Kim HI. Preparation of O/W Pickering emulsion with oxygen plasma treated carbon nanotubes as surfactants. *J Ind Eng Chem* 2011;17:455-460.
- [9] Kimmer D, Slobodian P, Petras D, Zatloukal M, Olejnik R, Saha P. Polyurethane/multiwalled carbon nanotube nanowebs prepared by an electrospinning process. *J Appl Polym Sci* 2009;111(6):2711-2714.
- [10] Harris PJF. Carbon nanotube science: synthesis, properties and applications, Cambridge University Press 2009, p.123.
- [11] Licea-Jimenez L, Henrio PY, Lund A, Laurie TM, Perez-Garcia SA, Nyborg L, Hassander H, Bertilsson H, Rychwalski RW, *Compos Sci Technol* 2007;67(5): 844-854.
- [12] Li Q, Ma Y, Mao C, Wu C. Grafting modification and structural degradation of multi-walled carbon nanotubes under the effect of ultrasonics sonochemistry. *Ultrason Sonochem* 2009;16(6):752-757.
- [13] Zhang J, Zou HL, Qing Q, Yang YL, Li QW, Liu ZF, Guo XY, Du ZL. Effect of

- chemical oxidation on the structure of single-walled carbon nanotubes. *J Phys Chem B* 2003;107(16):3712-3718.
- [14] Zhang J, Zou HL, Qing Q, Yang YL, Li QW, Liu ZF, Guo XY, Du ZL. Effect of chemical oxidation on the structure of single-walled carbon nanotubes. *J Phys Chem B* 2003;107(16):3712-3718.
- [15] Kastanis D, Tasis D, Papagelis K, Parthertios J, Tsakiroglou C, Galiotis C, Oxidized multi-walled carbon nanotube film fabrication and characterization, *Adv Compos Lett* 2007;16(6):243-248.
- [16] Allaoui A, Hoa SV, Evesque P, Bai J. Electronic transport in carbon nanotube tangles under compression: The role of contact resistance. *Scripta Mater* 2009;61(6):628-631.
- [17] Yeh CS. A Study of Nanostructure and Properties of Mixed Nanotube Buckypaper Materials: Fabrication, Process Modeling Characterization, and Property Modeling. The Florida State University USA, PhD Thesis;2007.
- [18] Slobodian P, Riha P., Saha P., A highly-deformable composite composed of an entangled network of electrically-conductive carbon-nanotubes embedded in elastic polyurethane, *Carbon* 2012;50:3446-3453.

## Figures

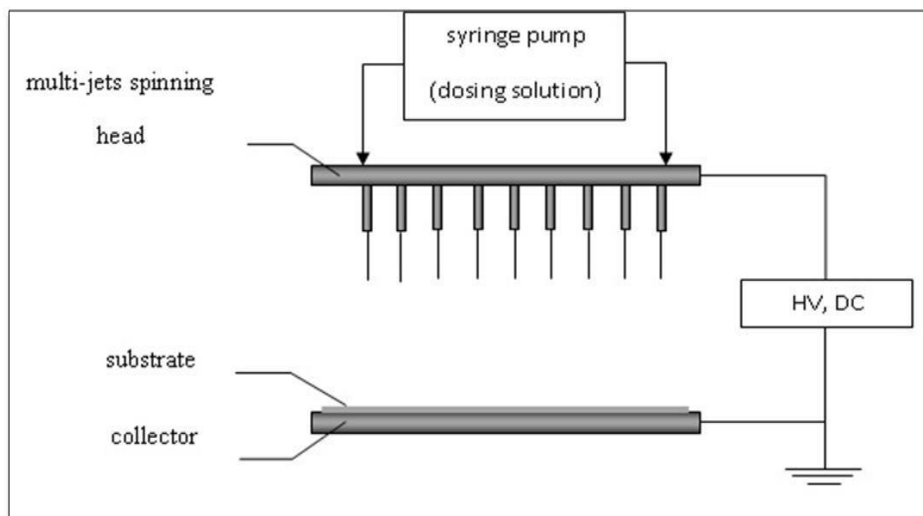


Fig. 1 Schematic diagram of the multi-jet electrospinning apparatus.

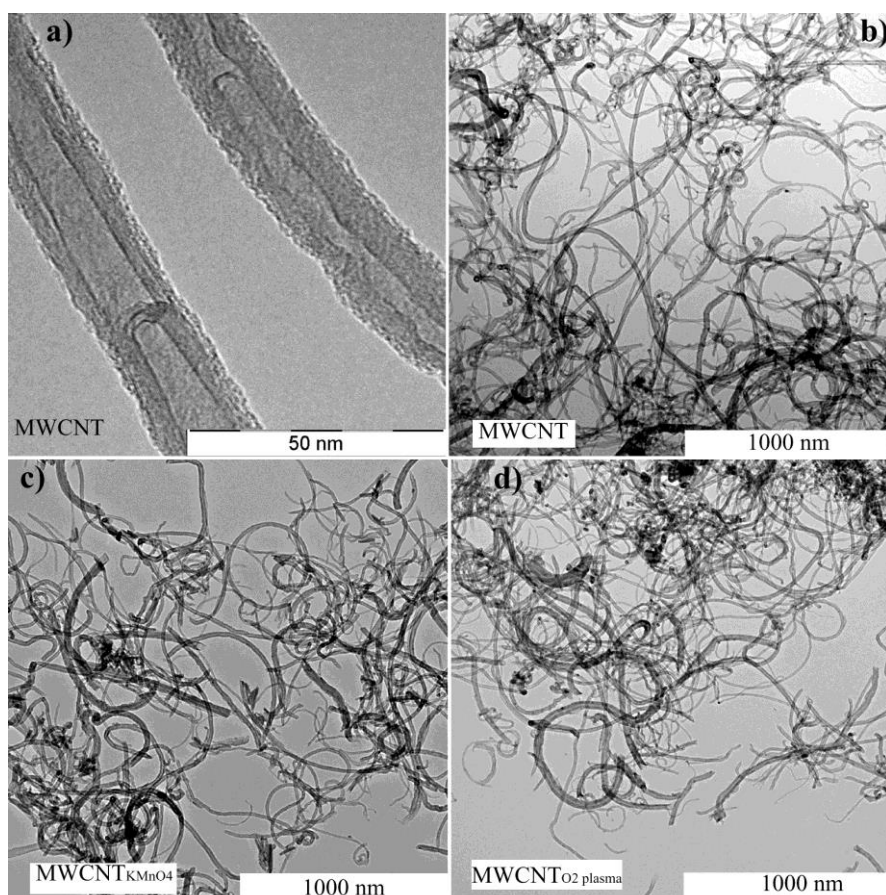


Fig. 2 a,b) TEM micrographs of pristine nanotubes (BAYTUBES C70 P), c)  $\text{KMnO}_4$  wet oxidized nanotubes, and d)  $\text{O}_2$  plasma shortened nanotubes.

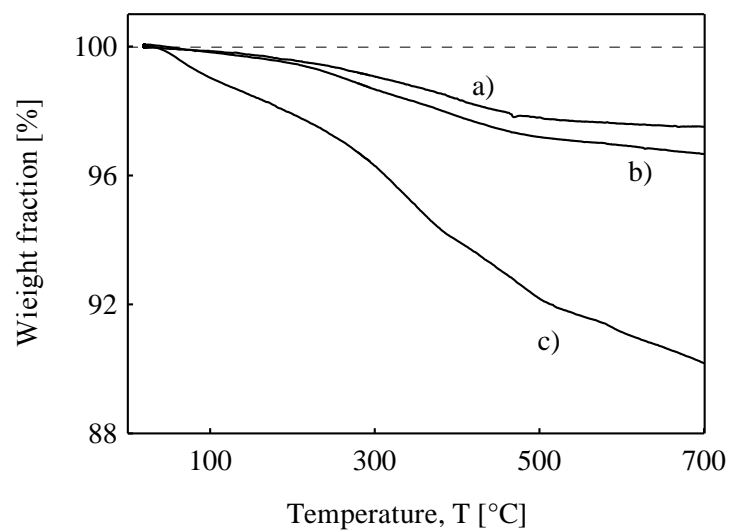


Fig. 3 Thermogravimetric analysis of nanotubes: a) pristine nanotubes (BAYTUBES C70 P), b) O<sub>2</sub> plasma shortened, c) KMnO<sub>4</sub> wet oxidized nanotubes.

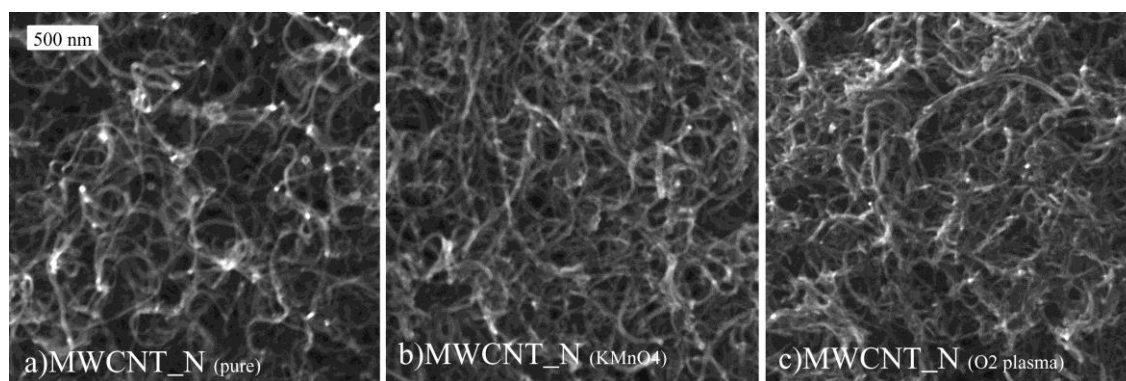


Fig. 4 SEM micrographs of the surface of entangled MWCNT network of pristine MWCNT (a), KMnO<sub>4</sub> oxidised MWCNT (b) and O<sub>2</sub> plasma shortened nanotubes (c).

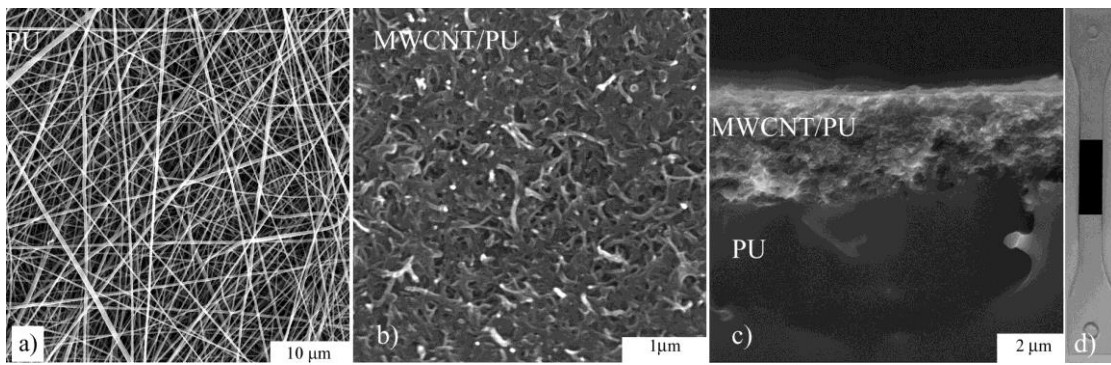


Fig. 5 SEM micrographs a) polyurethane non-woven filtering membrane; b) upper surface of MWCNT/PU composite layer after washing out the pure MWCNT network; c) cross-section through polyurethane base and MWCNT/PU composite layer; d) Photograph of PU dog-bone shaped specimen, for the tensile test, with the fixed stripe of MWCNT/PU composite (black).

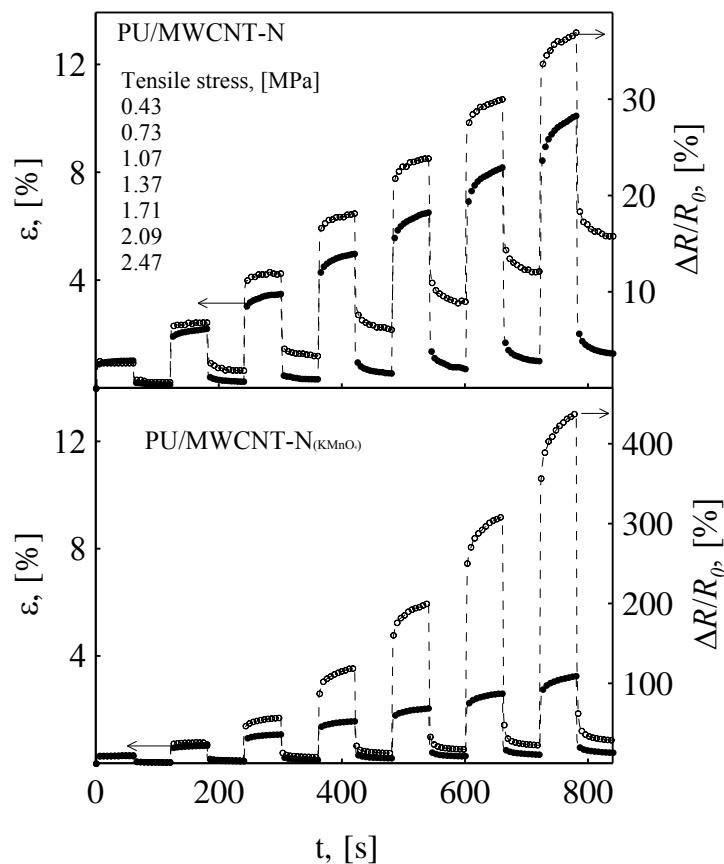


Fig. 6 Response of the relative resistance change,  $\Delta R/R_0$ , and the strain,  $\varepsilon$ , of MWCNT-N/PU and MWCNT-N<sub>(KMnO<sub>4</sub>)</sub>/PU composites to the step increase of tensile



stress as indicated in the graph. The strain values are denoted by solid circles, the relative resistance change by open circles.

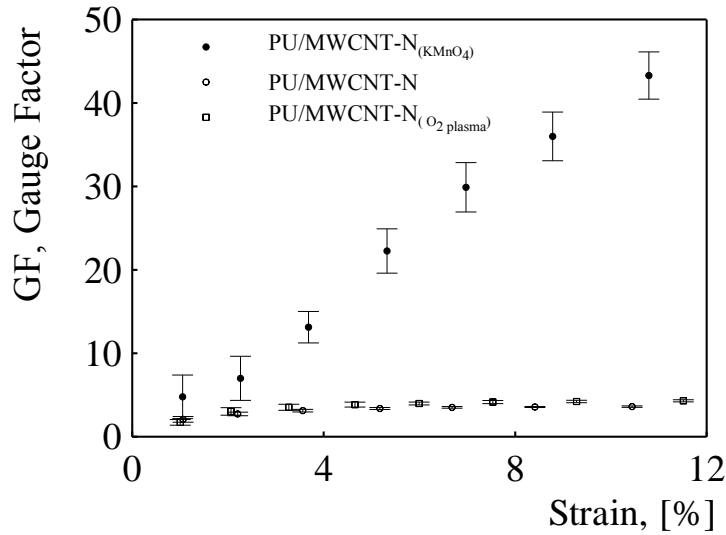


Fig. 7 Strain dependence of gauge factor  $GF$  of tested composites. The symbols represent means ( $n=5$ ) and the error bars show the standard deviation.

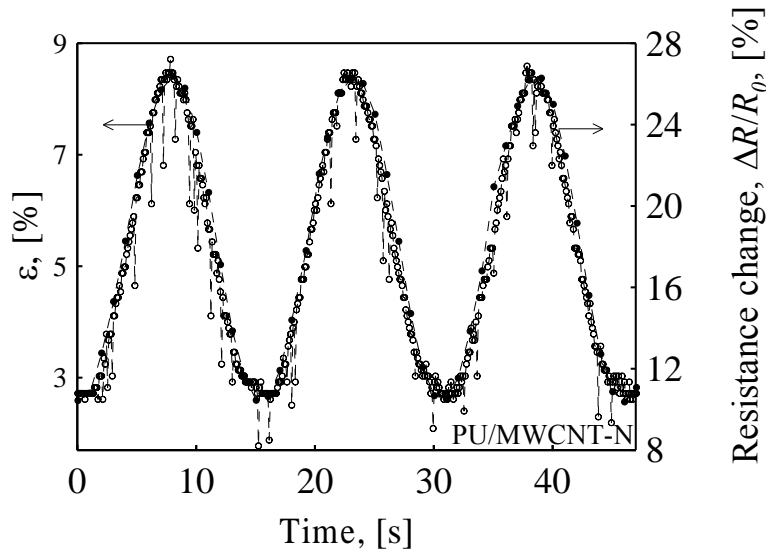


Fig. 8 Relative resistance change,  $\Delta R/R_0$ , induced by sinusoidal deformation for MWCNT-N/PU composite. The frequency of strain variation is  $\sim 0.07$  Hz. The strain values are denoted by solid circles, the relative resistance change by open circles.

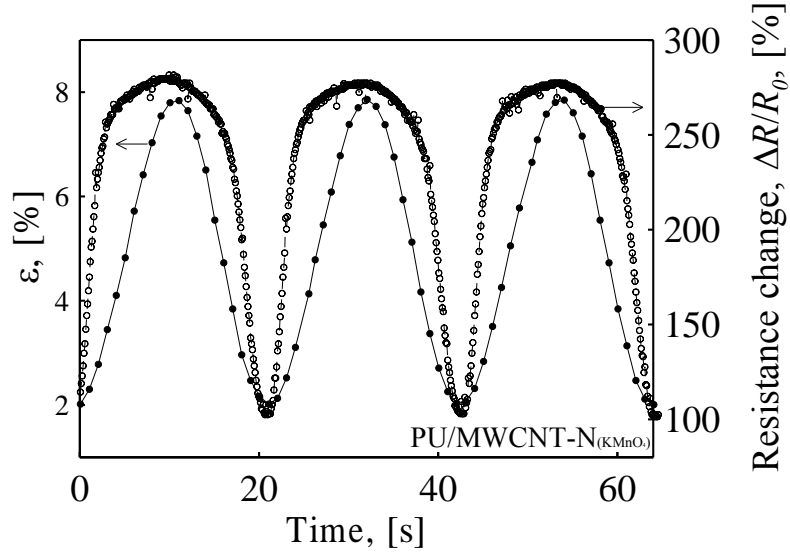


Fig. 9 Relative resistance change,  $\Delta R/R_0$ , induced by sinusoidal deformation for MWCNT- $N_{(KMnO_4)}$ /PU composite. The frequency of strain variation is  $\sim 0.05$  Hz. The strain values are denoted by solid circles, the relative resistance change by open circles.

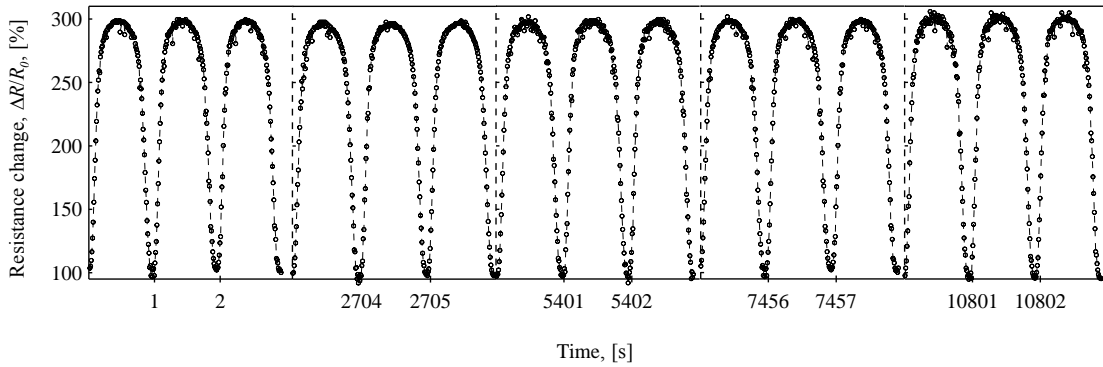


Fig. 10 The cyclic test of MWCNT- $N_{(KMnO_4)}$ /PU composite in more than  $10^4$  cycles. The strain varies between 2 % and 7.9 %, the frequency of strain variation is  $\sim 1.0$  Hz.